



# Integration of HYDRUS-1D and MODFLOW for evaluating the dynamics of salts and nitrogen in groundwater under long-term reclaimed water irrigation

Sidan Lyu<sup>1,2</sup> · Weiping Chen<sup>2</sup> · Xuefa Wen<sup>1</sup> · Andrew C. Chang<sup>3</sup>

Received: 17 April 2018 / Accepted: 6 October 2018 / Published online: 12 October 2018  
© Springer-Verlag GmbH Germany, part of Springer Nature 2018

## Abstract

Reclaimed water has been extensively used as an alternative resource for irrigation, but can affect groundwater quality due to salt and nitrogen leaching. We conducted field investigations of a shallow groundwater monitoring well at the Research Center for Eco-Environmental Sciences, China, and irrigated sample sites of turf grass with reclaimed water for 8 years. The HYDRUS-1D and MODFLOW models were integrated to study the transport and distribution of electrical conductivity ( $EC_{gw}$ ) and nitrate-N ( $N-NO_3^-$ ) in the shallow groundwater under long-term reclaimed water irrigation. Model calibration and validation showed that the integrated model could simulate the fates of  $EC_{gw}$  and  $N-NO_3^-$  in the shallow groundwater. Field experiments and the model simulation showed that reclaimed water irrigation can increase salinity and  $N-NO_3^-$  concentration in shallow groundwater and predicted, assuming the continuation of current irrigation practices, that the annual average  $EC_{gw}$  and  $N-NO_3^-$  would reach a steady level of  $0.72 \text{ dS m}^{-1}$  and  $2.18 \text{ mg L}^{-1}$ , respectively. Because  $EC_{gw}$  increased with increasing irrigation water salinity and amount, there is a risk of increased salinity in the shallow groundwater under long-term reclaimed water irrigation. Under all simulation scenarios, annual average  $N-NO_3^-$  concentrations in the shallow groundwater at an equilibrium state did not exceed the class II groundwater quality standard ( $2-5 \text{ mg L}^{-1}$ ). After proper calibration and validation, the integration of HYDRUS-1D and MODFLOW models offers an effective tool for analyzing irrigation management of low-quality water in water-scarce regions.

## Introduction

Reclaimed water has been an important element in urban water management (Brown et al. 2013) and has commonly been used for landscape or agricultural irrigation to compensate for a shortage of water supply (Cirelli et al. 2012). California and Florida have the largest water reuse programs

with reuse of approximately 500 million gallons per day (MGD), followed by Texas and Arizona with an average of 200 MGD in the United States (Tran et al. 2016). These four states account for 90% of the total water reuse in the country, which mainly is used as an environmental buffer (e.g. groundwater recharge, soil irrigation, and so on) (Sanchez-Flores et al. 2016). Australia uses 21% of its treated municipal wastewater, two-thirds of which is for irrigation (United Nations Environment Programme 2015). Israel as a global leader in terms of reclaimed water reuse, about 400 million  $\text{m}^3$ /year of treated wastewater was reused primarily for agriculture, and this constitutes about 40% of water use in agriculture (Kalavrouziotis et al. 2015). In China, 6000 million  $\text{m}^3$  of reclaimed water was reused in 2015, and the utilization ratio of reclaimed water exceeded 30% in Beijing; about 25% urban green spaces in Beijing are irrigated with reclaimed water (Sun et al. 2014; Zhu et al. 2018).

The quality of reclaimed water is dependent on the quality of the source water and the extent of treatment, and it may contain a fair amount of organic matter, plant nutrients, salts (i.e., dissolved minerals), and heavy metals (Wang

---

Communicated by A. Ben-Gal.

✉ Weiping Chen  
wpchen@rcees.ac.cn

<sup>1</sup> Key Laboratory of Ecosystem Network Observation and Modeling, Institute of Geographic Sciences and Natural Resources Research, Chinese Academy of Sciences, Beijing 100101, China

<sup>2</sup> State Key Laboratory of Urban and Regional Ecology, Research Center for Eco-Environmental Sciences, Chinese Academy of Sciences, Beijing 100085, China

<sup>3</sup> Department of Environmental Sciences, University of California, Riverside, CA 92521, USA

et al. 2018a). Used for irrigation, these constituents might be inadvertently introduced into the soils. Excessive and uncontrolled nitrogen inputs can lead to nutrition imbalance, affecting plant development (Pereira et al. 2011). Similarly, dissolved salts accumulating in the root zone can adversely affect soil physical properties, impeding water movement in soils and stunting plant growth from a high soil salinity (de Miguel et al. 2013; Pedrero et al. 2015). As the applied water leaches beyond the root zone, the potential risks for groundwater contamination increase (Gilabert-Alarcon et al. 2018). The dynamics of salts and nitrogen leaching and their concentration distributions in soil profiles and shallow groundwater have been studied in laboratories (Johnson et al. 1999; Lian et al. 2013) and in fields (Chen et al. 2006; Katz et al. 2009; Kass et al. 2005); however, these site- and case-specific outcomes have been unable to quantitatively predict the impact of long-term reclaimed water irrigation.

Mathematical models, such as HYDRUS-1D (Ramos et al. 2011; Simunek et al. 2016; Tafteh and Sepaskhah 2012) and ENVIRO-GRO (Chen et al. 2013), have been used for assessing the impacts of irrigation and fertilizer application by simulating the fate and transport of salts and nutrients in soil profiles. Water flow in the vadose zone is usually assumed to be vertically one-dimensional in the field. While capable of simulating the fate of solutes in the saturated zone, regional-scale groundwater models, such as MODFLOW, greatly simplify near-surface hydrologic processes (Xu and Shao 2002). Integration of a 1-D vadose zone flow model with a groundwater flow model through the exchange of information between the two presents an alternative method to simulate the fate and transport of salts and nitrogen and to assess the long-term impacts of irrigation with reclaimed water (Twarakavi et al. 2008; Xu et al. 2012).

In this study, we evaluated the risk of salt and nitrogen pollution of shallow groundwater due to long-term reclaimed water irrigation based on the results of a long-term field experiment and the integrated simulations of the HYDRUS-1D and MODFLOW models. We used data obtained from the long-term field experiment to calibrate and validate the simulations. The effects on groundwater pollution due to the amount and quality of irrigation water were evaluated subsequent to validation.

## Materials and methods

### Field experiments

A long-term field experiment was conducted at the Research Center for Eco-Environmental Sciences (RCEES), Chinese Academy of Sciences (40°00'28"N, 116°20'15"E) where one of the observation sites of the Beijing Urban Ecosystem Research Station is located. The area has a typical

monsoon-influenced humid continental climate, with a mean annual precipitation of 630 mm, a mean annual reference evapotranspiration of 1100 mm and a mean annual temperature of 13.3 °C (Liu et al. 2014a). More than 70% of the annual rains fall in July, August, and September. Soil types mainly include Fluvo-aquic soil and Cinnamon soil in the plain area, with soil pH ranges from 7.64 to 8.30 (Chen et al. 2013).

The site for the field experiment was an open green space planted with turf grass that was regularly mowed as needed. Prior to May 2006, the field was irrigated with local tap water, but after 2006, reclaimed water for irrigation came from the treated effluent of locally produced wastewater within the RCEES campus. Wastewater treatment consisted of granulated activated carbon filtration and ozonation. The field was sprinkle irrigated two to three times per week during the growing season from March to November for an annual amount of 330–530 mm. Irrigation applications were conducted with an amount of irrigation water that was about 1.1–1.3 times the annual potential  $ET_c$  between mid-March and mid-November. Irrigation rates were 10–15 mm/h. No fertilizer was applied. A shallow groundwater monitoring well was installed by the Beijing Urban Ecosystem Research Station to a depth of 6 m corresponding to a permeable layer.

Electrical conductivity (EC), nitrate-N ( $N-NO_3^-$ ), and ammonia-N ( $N-NH_4^+$ ) in groundwater were continually sampled and measured once a month from 2005 by the Beijing Urban Ecosystem Research Station. Simultaneously, groundwater levels were also continually measured once a month. Concentrations of EC,  $N-NO_3^-$ , and  $N-NH_4^+$  in the reclaimed water were added to the sampling regime in 2007. The electrical conductivity of the saturation extract ( $EC_e$ ) of soil sampled from a depth of 0–20 cm in 2011 and 2013 was measured for model calibration and validation. EC was measured with a Mettler Toledo 326 conductivity meter (Mettler Toledo Inc, Switzerland).  $N-NO_3^-$  was determined by ion chromatography using a Dionex ICS-1000 (Dionex, USA) ion chromatograph (Mou et al. 1993) and  $N-NH_4^+$  was determined by the spectrophotometric method using Nessler's reagent (Ministry of Environmental Protection of China 2002).

### Model simulation

#### Model description

The HYDRUS-1D software package (Simunek et al. 2008) simulates one-dimensional movement of water, heat, and multiple solutes in variably saturated porous media. The model numerically solves the Richards equation for variably saturated water flow and convective–dispersion equations for both heat and solute transport using the finite element method. The Visual MODFLOW software (Waterloo

Hydrogeologic Inc. 2006), a modular, three-dimensional, finite-difference groundwater flow model, predicts temporal changes of water flow and solutes in the groundwater. The solute transport in MODFLOW is solved by the Modular 3-Dimensional Transport model (MT3DMS), which is described based on the mass balance (Zheng and Wang 1999).

The integrated modeling approach between HYDRUS-1D and MODFLOW allows MODFLOW to receive drainage from HYDRUS-1D as recharge to the groundwater flow system, and assignment of pressure head as the bottom boundary condition in HYDRUS-1D as the calculated water table depth from MODFLOW (Twarakavi et al. 2008). The efficiency of an integrated vadose zone–groundwater model depends on the two models interacting with each other in space and time. The groundwater modeling domain for MODFLOW is discretized into grids or blocks, as described by Harbaugh et al. (2000), and these grids can be divided into zones based on similarities in soil hydrology and topographic characteristics. One HYDRUS soil profile is assigned to each of these zones. In the integrated HYDRUS-1D and MODFLOW system, proper treatment of water flow and solute equations require different time steps to solve the vadose zone and groundwater flow. In general, each MODFLOW time step consists of many HYDRUS time steps, and the bottom flux at each soil profile of HYDRUS is calculated for a net recharge flux at the start of each MODFLOW time step. The progress of water flow through the soil profile in the coupled model is shown schematically in Fig. 1.

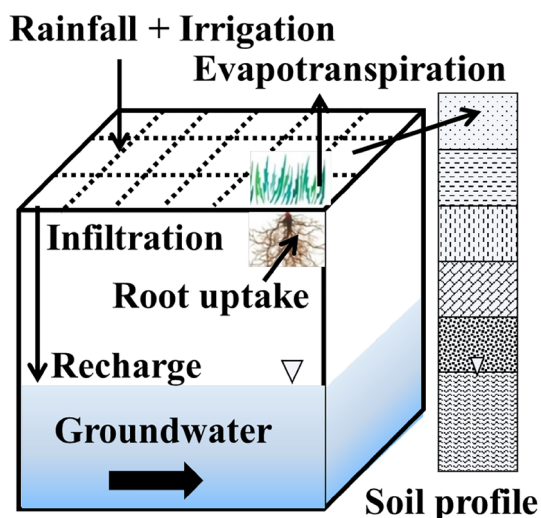


**Fig. 1** The progress of water flow through the soil profile in the coupled model

## Model parameters

The simulation domain was a landscape green space with an area of  $50 \times 50 \text{ m}^2$  and a depth of 16 m. For the simulation of EC, the period of calibration was from 2006 to 2012. The year 2013 was used for validation. To allow long-term prediction of EC, the daily meteorological data for 2013 were taken as the averaged data from 2006 to 2012. For the simulation of  $\text{N-NO}_3^-$  and  $\text{N-NH}_4^+$ , the period of calibration was 2012 and the period of validation was 2013 using the average daily meteorological data from 2006 to 2012. We set the period of model prediction to 10 years for a long-term simulation of EC,  $\text{N-NO}_3^-$  and  $\text{N-NH}_4^+$  in the shallow groundwater. The 300-cm soil profile in HYDRUS-1D was chosen and divided into five layers based on the soil physical and chemical characteristics. For the MODFLOW simulation, the flow domain was divided discretely into  $50 \times 50 \times 1$  grids. The model parameters and conditions obtained from the literature and field investigations are summarized as follows:

**HYDRUS-1D model Initial conditions** Initial conditions for the HYDRUS-1D model were specified in terms of soil water content, EC in soil water ( $\text{EC}_{\text{sw}}$ ), and concentrations of  $\text{N-NH}_4^+$  and  $\text{N-NO}_3^-$ . To obtain these initial values, laboratory analyses were performed on soil samples collected from the green space irrigated with tap water. Because  $\text{EC}_e$  was used in the model,  $\text{EC}_{1.5}$  needed to be transformed to  $\text{EC}_e$  based on the results of Li et al. (1996). The initial soluble concentrations determined in representative soil profiles are shown in Table 1.

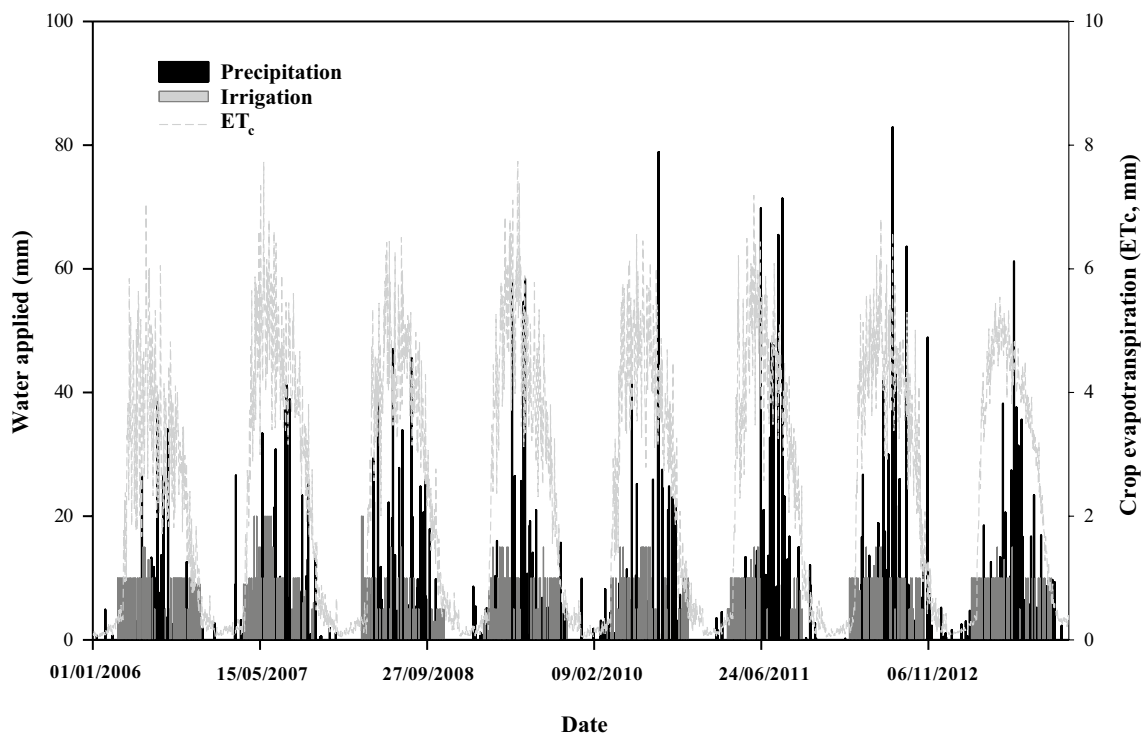
**Time-variable boundary conditions** Atmospheric and variable pressure head conditions were defined as the boundary conditions at the surface and bottom, respectively. Atmospheric boundary conditions were specified using meteorological data, from which daily values of the reference evapotranspiration rate ( $\text{ET}_0$ ) were calculated using the Penman–Monteith method (Allen et al. 1998). Crop evapotranspiration rates ( $\text{ET}_c$ ) were then calculated using the  $\text{ET}_0$  and crop coefficients ( $K_c$ ) from existing field observations (Allen et al. 1998; Yuan et al. 2009). As required by HYDRUS-1D,  $\text{ET}_c$  daily values were divided according to the growth stages of turf grasses (Chen et al. 2013) into two components: crop transpiration (T) and soil evaporation (E) rates. During the initial stage, turf grass is yet to turn green and ET was, therefore, set as E. After green-turning, the ground surface being covered by turf grass is more than 100% and ET was set as T.

Daily values of precipitation, irrigation, and crop evapotranspiration are presented in Fig. 2. Meteorological data from 2006 to 2012 were collected by the weather station, and values were averaged to obtain the meteorological data for 2013. The EC ( $\text{EC}_{\text{pw}}$ ) and concentrations of  $\text{N-NH}_4^+$  and  $\text{N-NO}_3^-$  in precipitation were set to  $0.05 \text{ dS m}^{-1}$ ,  $4 \text{ mg L}^{-1}$ ,

**Table 1** Soil physical and chemical characteristics for the HYDRUS-1D model

Property	Depth				
	0–20 cm	20–40 cm	40–60 cm	60–80 cm	80–300 cm
Bulk density ( $\text{g cm}^{-3}$ )	1.46	1.54	1.71	1.7	1.61
Sand (%)	54.4	52.71	45.97	41.11	42.93
Silt (%)	45.1	46.81	53.41	58.29	56.47
Clay (%)	0.49	0.48	0.62	0.6	0.6
Texture	Sandy loam	Sandy loam	Silt loam	Silt loam	Silt loam
$\theta_i$ ( $\text{cm}^3 \text{cm}^{-3}$ )	0.20	0.15	0.15	0.16	0.18
Initial $EC_e$ ( $\text{dS m}^{-1}$ )	0.61	0.67	0.73	0.90	0.77
Initial $\text{N-NO}_3^-$ ( $\text{mg L}^{-1}$ )	1.25	1.62	1.84	2.41	4.79
Initial $\text{N-NH}_4^+$ ( $\text{mg L}^{-1}$ )	0	0	0	0	0

$\theta_i$  initial water content,  $EC_e$  electrical conductivity of the saturated extract

**Fig. 2** Daily values of precipitation, irrigation, and crop evapotranspiration ( $ET_c$ ) from January 1, 2006 to December 31, 2013

and  $6 \text{ mg L}^{-1}$ , respectively, based on existing field observations (Xu and Han 2009; Wang et al. 2009). The observed concentrations of individual solutes in reclaimed water and tap water during the growing seasons are presented in Fig. 3.

**Soil hydraulic properties** The disturbed soil samples, after air drying and passing through a 2-mm sieve, were used for determination of particle size distribution by laser grain-size analysis (Konert and Vandenberghe 1997). Bulk density ( $\text{g cm}^{-3}$ ) was determined using the core method, as described by United States Salinity Laboratory Staff (1954). The undisturbed cylinder samples were collected from different soil layers to measure soil hydraulic

properties. Soil water retention curves were determined using a pressure plate apparatus (Klute 1986) between pressure heads of approximately  $-33$  and  $-1500$  kPa, and saturated hydraulic conductivity  $K_s$  was determined using a constant-head method (Stolte 1997). The parameters of the van Genuchten–Mualem equations (van Genuchten 1980) were optimized using simultaneous retention and conductivity data with the Retention Curve (RETc) computer program (van Genuchten et al. 1991). Soil hydraulic parameters are listed in Table 2. For every soil layer, identical soil hydraulic parameters were considered, thus

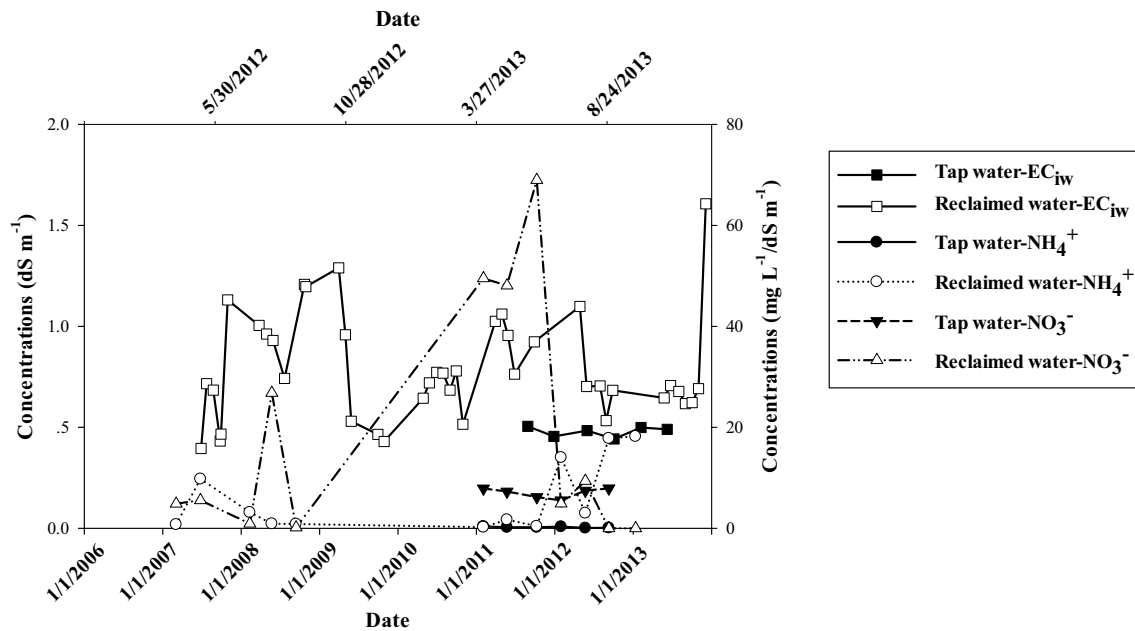


**Fig. 3** Concentrations of  $EC_{iw}$  (2007–2013),  $N-NH_4^+$  (2012–2013) and  $N-NO_3^-$  (2012–2013) in reclaimed water and  $EC_{iw}$ ,  $N-NH_4^+$  and  $N-NO_3^-$  in tap water (2013) during the growing seasons.  $EC_{iw}$  is electrical conductivity of irrigation water

**Table 2** Soil hydraulic parameters of the van Genuchten–Mualem function and solute transport parameters

Depth (cm)	0–20	20–40	40–60	60–80	80–300
$\theta_r$ ( $cm^3 cm^{-3}$ )	0.052	0.05	0.05	0.054	0.055
$\theta_s$ ( $cm^3 cm^{-3}$ )	0.4	0.39	0.37	0.37	0.39
$\alpha$ ( $cm^{-1}$ )	0.010	0.005	0.005	0.014	0.005
$n$	1.34	1.43	1.32	1.2	1.35
$K_s$ ( $cm^3 d^{-1}$ )	150	130	120	100	80
$\lambda$ (cm)	8	8	8	6	6
$EC_{sw}$					
$D_w$ ( $cm^2 d^{-1}$ )	0.864	0.864	0.864	0.864	0.864
$N-NO_3^-$ and $N-NH_4^+$					
$D_w$ ( $cm^2 d^{-1}$ )	2.32	2.32	2.32	2.32	2.32

$\theta_r$  residual water content,  $\theta_s$  saturated water content,  $K_s$  saturated hydraulic,  $\alpha$  inverse of the air-entry value or bubbling pressure,  $n$  pore-size distribution index,  $\lambda$  longitudinal dispersivity,  $D_w$  molecular diffusion coefficient

neglecting the probable effect of spatial variability of soil hydraulic properties on water flow and solute transport.

**Solute transport parameters** Dispersivity ( $\lambda$ ) and molecular diffusion coefficient values of  $EC_{sw}$ ,  $N-NH_4^+$ , and  $N-NO_3^-$  were initially set based on Chen et al. (2013), Ramos et al. (2011), and Ye et al. (2014), and then were specified during the model calibration (Table 2). The parameters  $K_d$ ,  $\mu_w$ ,  $\mu_s$ , and  $\gamma_w$  were initially set based on published data presented by Ramos et al. (2011) and Ye et al. (2014), and then were specified during the model calibration. In

the HYDRUS-1D model,  $N-NO_3^-$  and  $EC_{sw}$  were assumed to be present only in the dissolved phase (adsorption coefficient,  $K_d = 0 cm^3 d^{-1}$ ), while  $N-NH_4^+$  was assumed to adsorb to the solid phase using a distribution coefficient  $K_d$  of  $3.5 cm^3 d^{-1}$ . The first-order decay coefficients ( $\mu$ ), representing nitrification from  $N-NH_4^+$  to  $N-NO_3^-$ , were set to 0.1, 0.04, 0.04, 0.001, and 0.001 at depths of 0–20, 20–40, 40–60, 60–80, and 100 cm, respectively. The first-order decay coefficients ( $\gamma$ ), representing denitrification in the liquid phases, were set to 0.015, 0.01, 0.01, 0.001, and 0.001 at depths of 0–20, 20–40, 40–60, 60–80, and 100 cm, respectively.

**Root distribution and root uptake** Root distributions were described over the root zone using the normalized root density distribution function. Root development parameters were set based on the existing field observations (Chen et al. 2014; Yuan et al. 2009; Zhang 2001). The Feddes model (Feddes et al. 1978) was used to describe the effects of water stress on root water uptake with soil water pressure head parameters taken from the HYDRUS-1D internal database of turf grasses. The S-shaped function (van Genuchten 1987) was used to describe the effects of salinity stress on root water uptake. Root uptake for salts was considered to be zero. Root nutrient uptake was passive and equal to the product of the sink term  $S$  in the water flow equation and the concentration of solutes.

**MODFLOW model** In the simulation with MODFLOW, initial hydrogeologic parameters including hydraulic con-



ductivity, diffusion coefficient and longitudinal dispersivity were obtained from Cheng et al. (2010), and were specified during the model calibration. The hydraulic conductivity in the  $x$ ,  $y$ , and  $z$  direction ( $K_x$ ,  $K_y$ , and  $K_z$ ) was set as 50, 50, and 20  $\text{m day}^{-1}$ , respectively, and the specific yield ( $S_y$ ) was set as 0.2 based on the calibration results. For the simulation of EC in shallow groundwater ( $\text{EC}_{\text{gw}}$ ), the diffusion coefficient and longitudinal dispersivity (ratio of horizontal to longitudinal dispersivity was 0.1; ratio of vertical–longitudinal dispersivity was 0.024) were set as  $0.864 \text{ cm}^2 \text{ day}^{-1}$  and 5 m, respectively. For the simulation of  $\text{N-NO}_3^-$ , the diffusion coefficient and longitudinal dispersivity were set as  $2.32 \text{ cm}^2 \text{ day}^{-1}$  and 5 m (Chen et al. 2010). We used a stress period length of 15 days to enable simulation of the recharge season with a computational time step of 1 day. For the simulation of  $\text{EC}_{\text{gw}}$ , the initial  $\text{EC}_{\text{gw}}$  was  $0.698 \text{ dS m}^{-1}$  and the initial water table was 1.93 m in 2006. The initial concentration of  $\text{N-NO}_3^-$  was  $9.5 \text{ mg L}^{-1}$ , and the initial water table was 2.44 m in 2012. The recharge flux of  $\text{N-NH}_4^+$  from HYDRUS was 0; thus, the simulation of  $\text{N-NH}_4^+$  in MODFLOW was negligible. The outputs of HYDRUS-1D were used to define the upper boundary conditions in MODFLOW. We assigned the northwest boundary of the flow domain to be a constant head boundary based on the observed pressure head in the observation well. The southeast boundary was considered as a drain boundary and calculated based on 0.025% of the hydraulic gradient (Wang 2011). The no-flow boundary was defined as the bottom of the modeled domain.

### Statistical analysis

Model performance was evaluated by the root mean square error (RMSE) and the Nash–Sutcliffe modeling efficiency (NSE). The RMSE is given by

$$\text{RMSE} = \sqrt{\frac{\sum_{i=1}^n (O_i - P_i)^2}{n - 1}} \quad (1)$$

The Nash–Sutcliffe modeling efficiency (NSE) is commonly used for evaluating the agreement between simulated and observed data (Nash and Sutcliffe 1970) and is expressed as

$$\text{NSE} = 1 - \frac{\sum_{i=1}^n (P_i - O_i)^2}{\sum_{i=1}^n (O_i - \bar{O})^2} \quad (2)$$

where  $n$  is the total number of observations,  $O_i$  and  $P_i$  are the  $i_{\text{th}}$  values of the observed and the predicted dataset, respectively, and  $\bar{O}$  is the average of the observed values.

### Simulation scenarios

We simulated the following scenarios to evaluate the impacts of various factors on the  $\text{EC}_{\text{gw}}$  and the concentration of  $\text{N-NO}_3^-$  in the shallow groundwater.

**Default scenario** The irrigation of turf grasses using reclaimed water in the landscape green space of RCEES was set as the default scenario. The  $\text{EC}_{\text{iw}}$  and concentrations of  $\text{N-NH}_4^+$  and  $\text{N-NO}_3^-$  in the irrigation water were set as  $1.2 \text{ dS m}^{-1}$ ,  $8 \text{ mg L}^{-1}$ , and  $26 \text{ mg L}^{-1}$ , respectively, as reported for averaged reclaimed water quality in Beijing (Yang 2007; Deng and Yang 2009). We used the averaged meteorological data and irrigation amounts from 2006 to 2012 in RCEES for this scenario.

**Irrigation water quality** Three different levels of  $\text{EC}_{\text{iw}}$  were set to assess the effects of irrigation water salinity on the  $\text{EC}_{\text{gw}}$ . We used  $0.6 \text{ dS m}^{-1}$  to represent tap water salinity, and 1.2 and  $2.4 \text{ dS m}^{-1}$  to represent normal and extreme reclaimed water salinities (Yang 2007; Deng and Yang 2009). Based on the observed values of reclaimed water in Beijing (Yang 2007; Deng and Yang 2009), the concentrations of  $\text{N-NH}_4^+$  and  $\text{N-NO}_3^-$  were 0.2 and  $7 \text{ mg L}^{-1}$  in the tap water and 8 and  $26 \text{ mg L}^{-1}$  in the normal reclaimed water, respectively. In the extreme condition, the concentrations of  $\text{N-NH}_4^+$  and  $\text{N-NO}_3^-$  in the reclaimed water were 16 and  $52 \text{ mg L}^{-1}$ , respectively.

**Irrigation practice** An annual irrigation amount of 992 mm (including precipitation and reclaimed water irrigation, about 1.16 times the  $\text{ET}_c$ ) was set as the normal irrigation practice. Two additional irrigation levels,  $0.8 \times \text{ET}_c$  and  $1.5 \times \text{ET}_c$ , were used to evaluate the impacts of the deficit and excess irrigation, respectively, on the transport of EC,  $\text{N-NH}_4^+$ , and  $\text{N-NO}_3^-$  in the soil and shallow groundwater.

## Results and discussion

### Observed salinity and $\text{N-NO}_3^-$ concentration in the shallow groundwater

Results of observed  $\text{EC}_{\text{gw}}$  from 2006 to 2013 are shown in Fig. 4. Observed  $\text{EC}_{\text{gw}}$  fluctuated dramatically, with a minimum of  $0.47 \text{ dS m}^{-1}$  recorded in August 2006 and a maximum of  $1.15 \text{ dS m}^{-1}$  recorded in June 2008. We found a high correlation between  $\text{EC}_{\text{iw}}$  and  $\text{EC}_{\text{gw}}$  ( $R^2 = 0.97$ ). In particular, higher  $\text{EC}_{\text{iw}}$  resulted in a higher  $\text{EC}_{\text{gw}}$  in 2008 and 2011 (Figs. 3, 4). Compared to the annual average  $\text{EC}_{\text{gw}}$  of  $0.66 \text{ dS m}^{-1}$  in the shallow groundwater under tap water irrigation from May 2005 to May 2006, the annual average  $\text{EC}_{\text{gw}}$  under reclaimed water irrigation was much higher

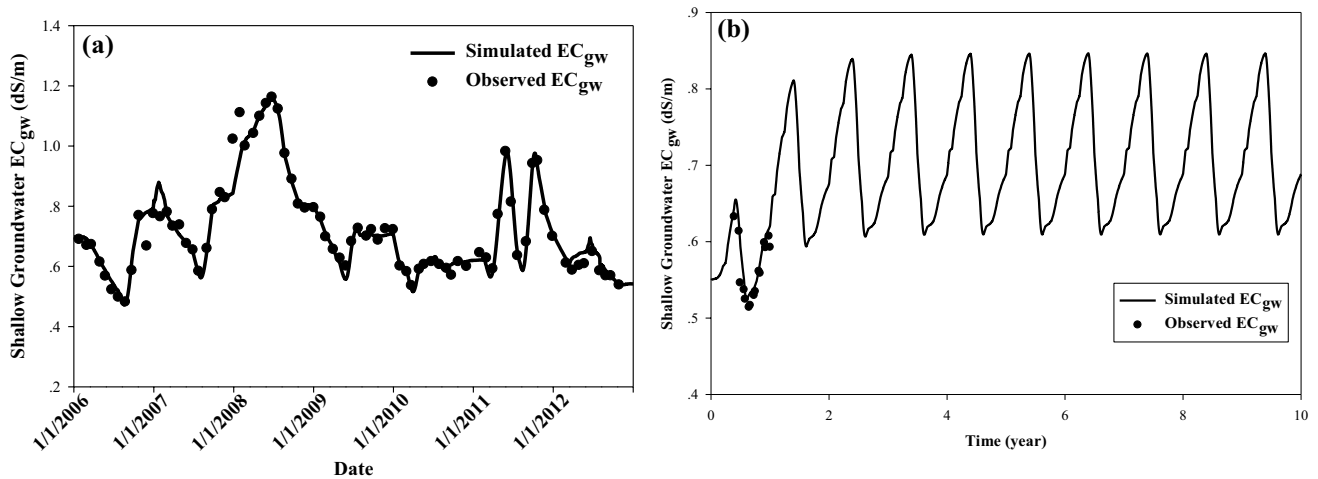


**Fig. 4** Simulated and observed salinity values in the shallow groundwater during the **a** calibration (2006–2012) and **b** validation (the first year, namely 2013) periods. In **b**, salinity in the shallow groundwater of RCEES was predicted based on the inputs of the model in 2013

except for 2010, 2012, and 2013, during which years dilution may have occurred from the higher levels of precipitation (Fig. 2). Based on US Salinity Laboratory (1954) criteria, the annual average EC<sub>gw</sub> in 2007, 2008, and 2011 was within the range of high-salinity water (EC 0.75–2.25 dS m<sup>-1</sup>) but in other years fell within the range of medium-salinity water (EC 0.25–0.75 dS m<sup>-1</sup>). Using the regression model of observed total dissolved solids (TDS) and EC<sub>gw</sub> (TDS mg L<sup>-1</sup> = 600 × EC<sub>gw</sub>, R<sup>2</sup> = 0.68) (Forkutsa et al. 2009), EC<sub>gw</sub> can be transformed to TDS for evaluating groundwater quality. Annual average TDS in the shallow groundwater in 2008 belonged to class-III groundwater quality (500–1000 mg L<sup>-1</sup>), while TDS in other years belonged to class-II groundwater quality according to Chinese standards (Ministry of Land and Resources of the People's Republic

of China 2015). Field observations demonstrated, therefore, that reclaimed water irrigation can increase salinity and result in the risk of salts polluting the shallow groundwater. Similarly, Wang et al. (2018b) measured hydrochemical characteristics in groundwater in the southeast irrigation region of Beijing, and found that the retained salts in soil after reclaimed water irrigation were greatly responsible for salinization of the local shallow aquifer.

The observed concentrations of N–NO<sub>3</sub><sup>-</sup> in the shallow groundwater in 2012 and 2013 are shown in Fig. 5. Annual average N–NO<sub>3</sub><sup>-</sup> in the shallow groundwater was 1.74 and 1.84 mg L<sup>-1</sup> in 2012 and 2013, respectively. The average values were less than 2 mg L<sup>-1</sup> and belonged to class-I groundwater quality based on the Chinese standard. However, observed concentrations of N–NO<sub>3</sub><sup>-</sup> in the shallow

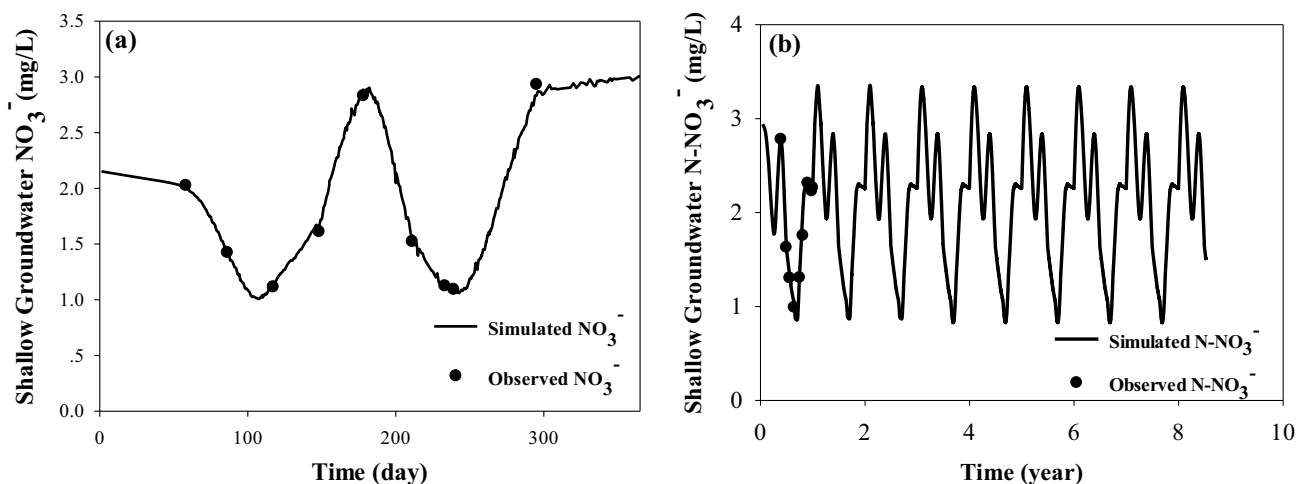


**Fig. 5** Simulated and observed N–NO<sub>3</sub><sup>-</sup> concentration in the shallow groundwater during the **a** calibration (2012) and **b** validation (the first year, namely 2013) periods. In **b** N–NO<sub>3</sub><sup>-</sup> concentration in the shallow groundwater was predicted based on the calibration in 2013

groundwater for some data points exceeded  $2 \text{ mg L}^{-1}$ , which placed these as class-II groundwater quality ( $2\text{--}5 \text{ mg L}^{-1}$ ). Variations in  $\text{N-NO}_3^-$  in the shallow groundwater showed similar variations with  $\text{N-NO}_3^-$  concentrations in the irrigation water. Under tap water irrigation from May 2005 to May 2006, the annual average  $\text{N-NO}_3^-$  concentration in the shallow groundwater was  $0.44 \text{ mg L}^{-1}$ , but this concentration increased obviously with the use of reclaimed water irrigation. The processes of rapid flushing and leaching during rain events or irrigation can promote the leaching of accumulated N through the unsaturated zone to the shallow groundwater (Liu et al. 2014b). Although  $\text{N-NO}_3^-$  concentration in the shallow groundwater was less than  $5 \text{ mg L}^{-1}$ , there remains a risk that reclaimed water irrigation could lead to nitrogen leaching to groundwater.

### Model calibration and validation

Coupled vadose zone–groundwater simulation in space and time through the vertical flow between the unsaturated soil profiles and the saturated aquifers can improve calculations of recharge and evapotranspiration fluxes varying with topography, soil type, land use, and water management practices. This, in turn, will improve the simulation of solute transport in the unsaturated–saturated aquifer (Liu et al. 2015; Zhu et al. 2012). Results of the statistical tests to investigate the performance of the integration of HYDRUS-1D and MODFLOW model are summarized in Table 3. During the calibration period for groundwater level and EC (from 2006 to 2012), the RMSE value was small and the NSE value was close to 1, indicating good agreement between the simulated and observed groundwater level and  $\text{EC}_{\text{gw}}$  by adjusting the solute transport parameters for HYDRUS and hydrogeologic parameters for MODFLOW (Figs. 4 and 6). For the validation period (2013), RMSE and NSE values suggested that the predicted groundwater level and  $\text{EC}_{\text{gw}}$  of the integrated model could be accepted (Figs. 4 and 6). Simulated soil salinities for the 0–20 cm soil profile during the calibration and validation periods are shown in Fig. 7. For the calibration, the difference between the simulated  $\text{EC}_e$  and observed  $\text{EC}_e$  in the soil was 0.5% in May 2011. For the validation, the difference between the simulated  $\text{EC}_e$  and observed  $\text{EC}_e$  in the soil was 0.4–0.9% in 2013. These results demonstrated that soil  $\text{EC}_e$  in the 0–20 cm soil profile were

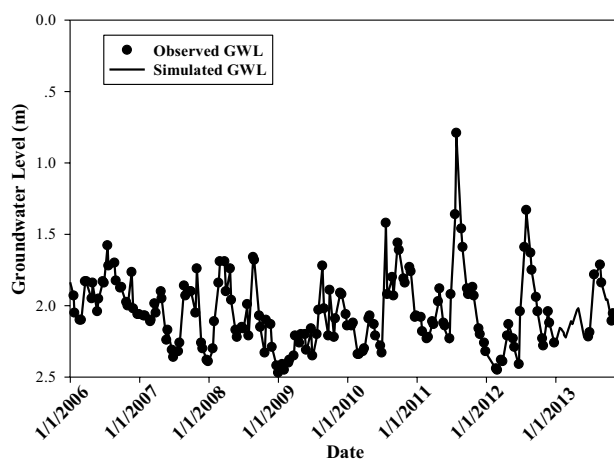


**Fig. 6** Simulated and observed groundwater level during the calibration (2006–2012) and validation (2013) periods

simulated well by HYDRUS-1D. For nitrogen, observed  $\text{N-NO}_3^-$  concentrations in the shallow groundwater in 2012 and 2013 were used for the calibration and validation, respectively (Fig. 5). Similar to the results of EC, RMSE values were small and NSE values were close to 1 as shown in Table 3, indicating that the integrated model successfully simulated the transport of  $\text{N-NO}_3^-$  in soil and groundwater.

### Annual change in salinity and $\text{N-NO}_3^-$ concentrations in the shallow groundwater

Under the default scenario, the changes predicted for  $\text{EC}_{\text{gw}}$  at RCEES after 10 years were simulated (Fig. 4b). With an increasing number of years of irrigation, the annual average  $\text{EC}_{\text{gw}}$  increased from  $0.58$  to  $0.72 \text{ dS m}^{-1}$ , with equilibrium reached in year 6. Because the same irrigation practices continued, the amount of salt applied would finally equal to the amount of salt removed by leaching, reaching equilibrium in terms of salinity levels. However, due to natural variations in climate between years, the actual state of equilibrium state would be unexpected (Chen et al. 2010).

Because the annual change to the EC of the reclaimed water during the growing season was small in 2013 (Fig. 3), we expected the amount of irrigation to play a key role in the annual change of  $\text{EC}_{\text{gw}}$ . The amount of irrigation with reclaimed water increased gradually from January to June

**Table 3** Results of the statistical analysis between observed and simulated groundwater level, electrical conductivity ( $\text{EC}_{\text{gw}}$ ) and  $\text{N-NO}_3^-$  concentration in the shallow groundwater

Statistics	Groundwater level		$\text{EC}_{\text{gw}}$		$\text{N-NO}_3^-$	
	Calibration	Validation	Calibration	Validation	Calibration	Validation
RMSE	0.18	0.22	0.04	0.03	0.20	0.13
NSE	0.86	0.83	0.95	0.86	0.99	0.99

*RMSE* root mean square error; the unit for RMSE is the unit of a particular variable. *NSE* Nash–Sutcliffe modeling efficiency



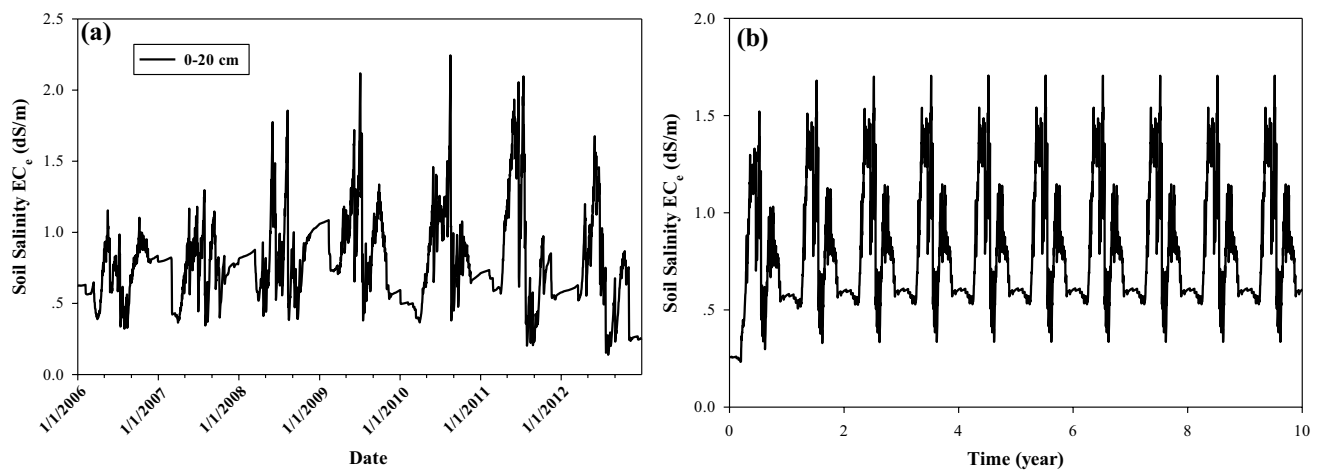


**Fig. 7** Simulated soil salinity at the 0–20 cm soil profile during the **a** calibration (2006–2012) and **b** validation (2013) periods. In **b**, soil salinity was predicted based on the calibration in 2013

and then decreased from July to October as rainfall increased and evaporative demand decreased. Corresponding to the change in irrigation water amount,  $EC_{gw}$  followed a pattern of first increasing and then decreasing at the equilibrium state. Less irrigation water and more ET caused the  $EC_{gw}$  to increase slightly in November and December due to a decreasing groundwater level. Similarly, the results of Wang et al. (2018b), from a reclaimed water irrigation region of Beijing, showed that reclaimed water leaching, together with dilution effects of rain, played a vital role in seasonal variation in shallow groundwater hydrochemistry.

For 39% of the days per year,  $EC_{gw}$  at equilibrium was classified as high-salinity ( $EC$  0.75–2.25  $dS\ m^{-1}$ ). The average and maximum annual TDS in the shallow groundwater at equilibrium were 431 and 505  $mg\ L^{-1}$ , respectively. Based on the irrigation conditions of 2013 at RCEES, the results indicated that there was a low salinity risk to shallow groundwater under long-term reclaimed water irrigation, though the  $EC_{gw}$  would increase as the number of years of irrigation increased.

The simulated results of  $N-NO_3^-$  in the shallow groundwater under the default scenario after 10 years of reclaimed water irrigation are shown in Fig. 5b. Annual average  $N-NO_3^-$  increased from 2.07 to 2.18  $mg\ L^{-1}$  as the number of years of irrigation increased, and the equilibrium state was reached in year 6. At the equilibrium state, two high peaks of  $N-NO_3^-$  concentration per year were evident. The first peak may be due to greater ET and less irrigation water in the winter, while higher nitrogen concentrations in the reclaimed water may have caused the second peak in May. In July and August,  $N-NO_3^-$  in the shallow groundwater decreased sharply because of heavy precipitation (Jang et al. 2012). Overall, annual average  $N-NO_3^-$  concentrations in the shallow groundwater fell into class-II water quality

(2–5  $mg\ L^{-1}$ ), indicating a low risk of  $N-NO_3^-$  polluting the shallow groundwater at RCEES, although  $N-NO_3^-$  concentrations in the shallow groundwater increased with long-term reclaimed water irrigation.

### Ecological risks of salinization and nitrate contamination with long-term reclaimed water irrigation

#### Salinity in the shallow groundwater

Irrigation practices, including irrigation water quality and amount, are important considerations for assessing the ecological risks of the salinization of the shallow groundwater under long-term reclaimed water irrigation. Simulated salinities in the shallow groundwater under three different conditions of irrigation water quality ( $EC_{iw} = 0.6, 1.2,$  and  $2.4\ dS\ m^{-1}$ ) for 10 years are shown in Fig. 8a.  $EC_{gw}$  increased with an increasing number of years of irrigation, and equilibrium was reached in year 6. At the equilibrium state, the annual average  $EC_{gw}$  increased by 21%, 31%, and 52%, respectively, compared with the annual average  $EC_{gw}$  in 2012 for the three water qualities. The results indicate that a higher  $EC_{iw}$  could result in a greater increase in  $EC_{gw}$ .

Under irrigation with tap water ( $EC_{iw} = 0.6\ dS\ m^{-1}$ ), the annual average  $EC_{gw}$  at equilibrium was 0.706  $dS\ m^{-1}$  [medium-salinity water class ( $EC$  0.25–0.75  $dS\ m^{-1}$ )], and annual average and maximum TDS in the shallow groundwater were 420 and 489  $mg\ L^{-1}$ , respectively (class-II groundwater quality). With irrigation using normal reclaimed water, the annual average  $EC_{gw}$  at equilibrium was 0.761  $dS\ m^{-1}$ , which is categorized as high-salinity ( $EC$  0.75–2.25  $dS\ m^{-1}$ ). Annual average and maximum TDS in the shallow groundwater at the equilibrium state were 457 and 525  $mg\ L^{-1}$ ,

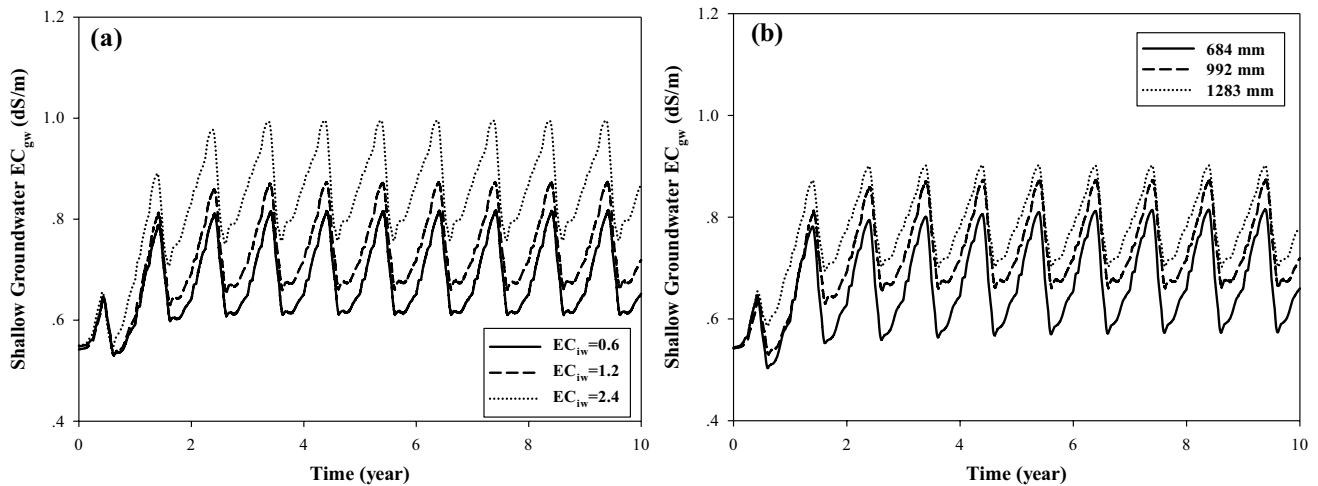


**Fig. 8** Temporal change of salinity in the shallow groundwater **a** under different irrigation water qualities and **b** under different irrigation amounts

respectively. These results placed the annual average TDS in class-II groundwater quality. However, for 25% of the days per year, TDS fell into class-III groundwater quality when irrigation water quality was  $1.2 \text{ dS m}^{-1}$ . With the extreme salinity condition at equilibrium, annual average  $\text{EC}_{\text{gw}}$  was  $0.876 \text{ dS m}^{-1}$  [high-salinity water ( $\text{EC } 0.75\text{--}2.25 \text{ dS m}^{-1}$ )] and the annual average and maximum TDS in the shallow groundwater were  $523$  and  $596 \text{ mg L}^{-1}$ , respectively (class-III groundwater quality). Therefore, there is a risk of salinity increasing in the shallow groundwater under long-term reclaimed water irrigation as the salinity in the irrigation water increases.

Because leaching is an important factor affecting salinity in soil and groundwater (Gilbert-Alarcon et al. 2018), three annual irrigation amounts (684, 992, and 1283 mm) were evaluated with the reclaimed water quality of  $1.2 \text{ dS m}^{-1}$ . The temporal change in  $\text{EC}_{\text{gw}}$  under different irrigation amounts is shown in Fig. 8b. The annual average  $\text{EC}_{\text{gw}}$  increased as the number of years of irrigation increased, and equilibrium was reached in year 6. At equilibrium, the annual average  $\text{EC}_{\text{gw}}$  levels were 0.686, 0.761, and  $0.802 \text{ dS m}^{-1}$ , respectively, for the three irrigation amounts, and these levels increased by 18%, 31%, and 39%, respectively, compared with the annual average  $\text{EC}_{\text{gw}}$  in 2012. Overall,  $\text{EC}_{\text{gw}}$  increased with increasing irrigation amount while soil  $\text{EC}_e$  decreased. An increasing amount of irrigation water increased the downward leaching of salinity, which resulted in increased salinity in the shallow groundwater and a decrease in salinity accumulation in the soil.

Using the water-saving irrigation amount of 684 mm, the annual average  $\text{EC}_{\text{gw}}$  at equilibrium was classified as medium-salinity, although for 25% of the days per year, the  $\text{EC}_{\text{gw}}$  had levels within the range of high-salinity water. Based on the conditions of the equilibrium state, the annual

average and maximum TDS in the shallow groundwater were  $412$  and  $489 \text{ mg L}^{-1}$ , respectively (class-II groundwater quality). With an excessive irrigation amount of 1283 mm, the annual average  $\text{EC}_{\text{gw}}$  at equilibrium was classified as high-salinity, and the annual average and maximum TDS in the shallow groundwater were  $481 \text{ mg L}^{-1}$  and  $543 \text{ mg L}^{-1}$ , respectively. In this case, the annual average TDS was classified as class-II groundwater quality, but for 32% of the days, the TDS fell into class-III groundwater quality. The results show a risk of increasing salinity in shallow groundwater under long-term reclaimed water irrigation as the amount of irrigation water increases.

#### N- $\text{NO}_3^-$ concentration in the shallow groundwater

The effects of irrigation water quality on N- $\text{NO}_3^-$  concentration in the shallow groundwater are shown in Fig. 9a. Annual average N- $\text{NO}_3^-$  concentration in the shallow groundwater increased as the number of years of irrigation increased, regardless of the irrigation water quality level used, and equilibrium was reached in year 6. At equilibrium, the annual average N- $\text{NO}_3^-$  concentrations in the shallow groundwater were 2.15, 2.16, and  $2.17 \text{ mg/L}$  and increased by 23%, 24%, and 24% with irrigation by tap water, normal reclaimed water, and extreme reclaimed water, respectively, compared with the annual average in 2012. Overall, annual average N- $\text{NO}_3^-$  concentration in the shallow groundwater at the equilibrium state fell into class-II groundwater quality for all three levels of irrigation water quality, and groundwater concentration increased slightly with increasing N- $\text{NO}_3^-$  concentration in the irrigation water.

We found a minimal effect of irrigation water amount on N- $\text{NO}_3^-$  concentration in the shallow groundwater. The annual average N- $\text{NO}_3^-$  concentrations in the shallow

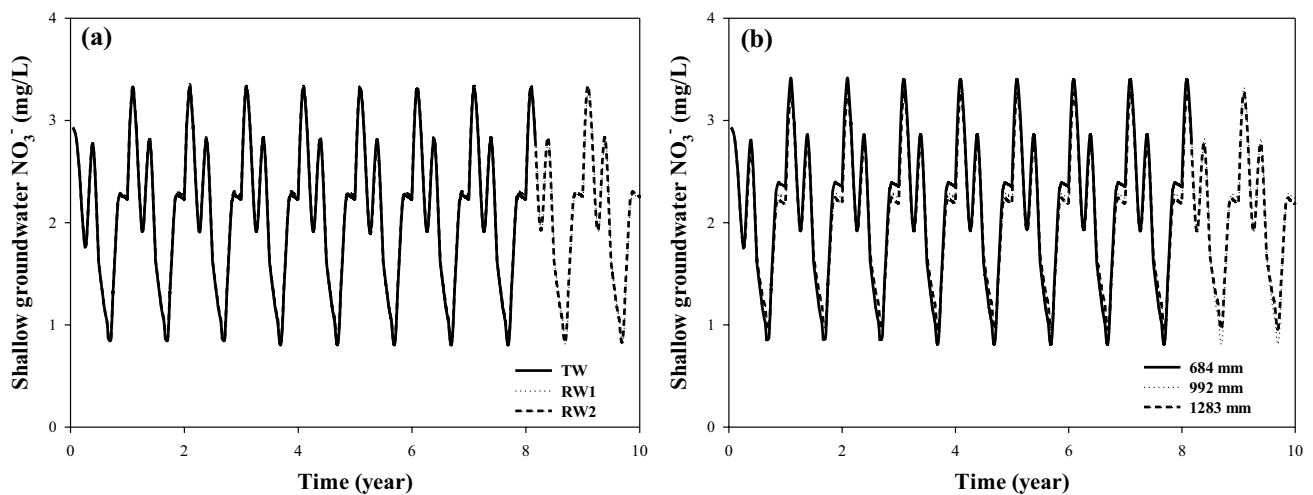


**Fig. 9** Temporal change of  $\text{N-NO}_3^-$  concentration in the shallow groundwater **a** under different irrigation water quality levels and **b** under different irrigation amounts

groundwater increased as the number of years of irrigation increased under the three cases, and equilibrium was reached in year 6. At equilibrium, the annual average  $\text{N-NO}_3^-$  concentrations in the shallow groundwater were 2.21, 2.16, and 2.17  $\text{dS m}^{-1}$  and increased by 26%, 24%, and 24% with 684, 992, and 1283 mm of irrigation water, respectively, compared with the annual average in 2012, and all annual average  $\text{N-NO}_3^-$  concentrations were classified as class-II groundwater quality.  $\text{N-NO}_3^-$  concentration in the shallow groundwater was slightly higher than the normal condition at the lowest amount of irrigation water (684 mm), most likely because the lower amount of water leaching was insufficient to dilute the  $\text{N-NO}_3^-$  concentration in the groundwater under these conditions (Wang et al. 2018b).

Factors affecting the temporal changes of  $\text{N-NO}_3^-$  concentration in the shallow groundwater with irrigation from reclaimed water included concentrations of  $\text{N-NH}_4^+$  and  $\text{N-NO}_3^-$  in the irrigation water, irrigation water amount, rates of nitrification and denitrification,  $\text{N-NO}_3^-$  upstream input, and root uptake (Lyu and Chen 2016). Overall, the impacts of irrigation water quality and amount on  $\text{N-NO}_3^-$  concentrations in the shallow groundwater were slight and represented a low risk of  $\text{N-NO}_3^-$  polluting the shallow groundwater. Xiao et al. (2017) found similar results in an investigation of groundwater quality in a typical long-term reclaimed water use area of Beijing.

## Conclusions

We used a field experiment and an integration of HYDRUS-1D and MODFLOW model to evaluate the ecological risks of salinization and nitrate contamination in the shallow groundwater under long-term reclaimed

water irrigation. Field experiments showed that the annual average  $\text{EC}_{\text{gw}}$  under reclaimed water irrigation was much higher except for the years 2010, 2012, and 2013, compared with the annual average  $\text{EC}_{\text{gw}}$  under tap water irrigation conditions. We found the amount of precipitation and irrigation and the  $\text{EC}_{\text{iw}}$  to be important factors affecting  $\text{EC}_{\text{gw}}$  under reclaimed water irrigation. Observed annual average  $\text{N-NO}_3^-$  in the shallow groundwater under reclaimed water irrigation was less than  $2 \text{ mg L}^{-1}$ , but this was higher than the concentration under tap water irrigation. Statistical analysis between observed and simulated values during the calibration and validation periods demonstrated that the integrated model successfully simulated the fates of salts and nitrogen between soil and groundwater.

The impacts of using reclaimed water for irrigation depend on its chemical makeup and quantity. Long-term use of reclaimed water with high salinity levels, and high water quantity can all result in TDS levels falling into class-III groundwater quality for a portion of the year. This is not the case for  $\text{N-NO}_3^-$ , which appears to have a low risk of polluting the shallow groundwater under conditions of high nitrogen concentration or high amounts of irrigation water. The risk of salt pollution compared to nitrogen pollution of the shallow groundwater is of even greater concern under long-term reclaimed water irrigation. In addition, our findings show that the comprehensive use of field experiments and the integration model of HYDRUS-1D and MODFLOW based on site-specific management conditions is an effective and powerful tool and can lead to limiting salinization and nitrate contamination in the groundwater and soil.

**Acknowledgements** We thank the National Natural Science Foundation of China (#41571130043) for its support.

## Compliance with ethical standards

**Conflict of interest** On behalf of all authors, the corresponding author states that there is no conflict of interest.

## References

- Allen RG, Pereira LS, Raes D, Smith M (1998) Crop evapotranspiration guidelines for computing crop water requirements. FAO irrigation and drainage paper 56. FAO, Rome
- Brown TC, Foti R, Ramirez JA (2013) Projected freshwater withdrawals in the United States under a changing climate. *Water Resour Res* 49(3):1259–1276. <https://doi.org/10.1002/wrcr.20076>
- Chen J, Tang C, Yu J (2006) Use of  $^{18}\text{O}$ ,  $^2\text{H}$  and  $^{15}\text{N}$  to identify nitrate contamination of groundwater in a wastewater irrigated field near the city of Shijiazhuang, China. *J Hydrol* 326(1–4):367–378. <https://doi.org/10.1016/j.jhydrol.2005.11.007>
- Chen W, Hou Z, Wu L, Liang Y, Wei C (2010) Evaluating salinity distribution in soil irrigated with saline water in arid regions of northwest China. *AGR Water Manag* 97(12):2001–2008. <https://doi.org/10.1016/j.agwat.2010.03.008>
- Chen W, Lu S, Pan N, Jiao W (2013) Impacts of long-term reclaimed water irrigation on soil salinity accumulation in urban green land in Beijing. *Water Resour Res* 49(11):7401–7410. <https://doi.org/10.1002/wrcr.20550>
- Chen LL, Yuan ZY, Shao HB, Wang DX, Mu XM (2014) Effects of thinning intensities on soil infiltration and water storage capacity in a Chinese pine-oak mixed forest. *Sci World J* 2014:1–7. <https://doi.org/10.1155/2014/268157>
- Cheng DH, Liu MZ, Chen HH, He JT, He GP, Lin J (2010) The hydro-geochemical modeling for total hardness in aquifer of urban area. In: 2010 4th international conference on bioinformatics and biomedical engineering, Chengdu, China. IEEE, pp 1–4
- Cirelli GL, Consoli S, Licciardello F, Aiello R, Giuffrida F, Leonardi C (2012) Treated municipal wastewater reuse in vegetable production. *AGR Water Manag* 104:163–170. <https://doi.org/10.1016/j.agwat.2011.12.011>
- de Miguel A, Martinez-Hernandez V, Leal M, Gonzalez-Naranjo V, de Bustamante I, Lillo J, Martin I, Salas JJ, Palacios-Diaz MP (2013) Short-term effects of reclaimed water irrigation: *Jatropha curcas* L. cultivation. *Ecol Eng* 50:44–51. <https://doi.org/10.1016/j.ecoleng.2012.06.028>
- Deng JF, Yang LX (2009) Irrigation security of reclaimed water based on water quality in Beijing. In: 2009 3rd international conference on bioinformatics and biomedical engineering, Beijing, China. IEEE, pp 1–4
- Feddes RA, Kowalik PJ, Zaradny H (1978) Simulation of field water use and crop yield. Wiley, New York
- Forkutsa I, Sommer R, Shirokova YI, Lamers JPA, Kienzler K, Tischbein B, Martius C, Vlek PLG (2009) Modeling irrigated cotton with shallow groundwater in the Aral sea basin of Uzbekistan: I. Water dynamics. *Irrig SCI* 27(4):331–346. <https://doi.org/10.1007/s00271-009-0148-1>
- Gilabert-Alarcon C, Daessle LW, Salgado-Mendez SO, Perez-Flores MA, Knoller K, Kretschmar TG, Stumpp C (2018) Effects of reclaimed water discharge in the Maneadero coastal aquifer, Baja California, Mexico. *Appl Geochem* 92:121–139. <https://doi.org/10.1016/j.apgeochem.2018.03.006>
- Harbaugh AW, Banta ER, Hill MC, McDonald MG (2000) MODFLOW-2000, the US geological survey modular groundwater model user guide to modularization concepts and the groundwater flow process. USGS, Denver
- Jang TI, Kim HK, Seong CH, Lee EJ, Park SW (2012) Assessing nutrient losses of reclaimed wastewater irrigation in paddy fields for sustainable agriculture. *AGR Water Manag* 104:235–243. <https://doi.org/10.1016/j.agwat.2011.12.022>
- Johnson JS, Baker LA, Fox P (1999) Geochemical transformations during artificial groundwater recharge: soil–water interactions of inorganic constituents. *Water Res* 33(1):196–206. [https://doi.org/10.1016/S0043-1354\(98\)00195-X](https://doi.org/10.1016/S0043-1354(98)00195-X)
- Kalavrouziotis IK, Kokkinos P, Oron G, Fatone F, Bolzonella D, Vatyliotou M, Fatta-Kassinos D, Koukoulakis PH, Varnavas SP (2015) Current status in wastewater treatment, reuse and research in some mediterranean countries. *Desalin Water Treat* 53(8):2015–2030. <https://doi.org/10.1080/19443994.2013.860632>
- Kass A, Gavrieli I, Yechieli Y, Vengosh A, Starinsky A (2005) The impact of freshwater and wastewater irrigation on the chemistry of shallow groundwater: a case study from the Israeli coastal aquifer. *J Hydrol* 300(1–4):314–331. <https://doi.org/10.1016/j.jhydrol.2004.06.013>
- Katz BG, Griffin DW, Davis JH (2009) Groundwater quality impacts from the land application of treated municipal wastewater in a large karstic spring basin: chemical and microbiological indicators. *Sci Total Environ* 407(8):2872–2886. <https://doi.org/10.1016/j.scitotenv.2009.01.022>
- Klute A (1986) Methods of soil analysis, Part 1: physical and mineralogical properties, monograph 9. American Society of Agronomy, Madison
- Konert M, Vandenberghe J (1997) Comparison of laser grain size analysis with pipette and sieve analysis: a solution for the underestimation of the clay fraction. *Sedimentology* 44(3):523–535. <https://doi.org/10.1046/j.1365-3091.1997.d01-38.x>
- Li DS, Yang JS, Zhou J (1996) Measure and conversion of electrical conductivity of the salt affected soil extracts in the Huanghuaihai plain. *Chin J Soil Sci* 27(6):285–287 (in Chinese)
- Lian J, Luo Z, Jin M (2013) Transport and fate of bacteria in SAT system recharged with recycling water. *Int Biodeterior Biodegrad* 76:98–101. <https://doi.org/10.1016/j.ibiod.2012.06.012>
- Liu HJ, Li Y, Josef T, Zhang RH, Huang GH (2014a) Quantitative estimation of climate change effects on potential evapotranspiration in Beijing during 1951–2010. *J Geogr Sci* 24(1):93–112. <https://doi.org/10.1007/s11442-014-1075-5>
- Liu M, Seyf-Laye ASM, Ibrahim T, Gbandi DB, Chen H (2014b) Tracking sources of groundwater nitrate contamination using nitrogen and oxygen stable isotopes at Beijing area, China. *Environ Earth Sci* 72(3):707–715
- Liu Y, Kuang XX, Jiao JJ, Li J (2015) Numerical study of variable-density flow and transport in unsaturated–saturated porous media. *J Contam Hydrol* 182:117–130. <https://doi.org/10.1016/j.jconhyd.2015.09.001>
- Lyu SD, Chen WP (2016) Soil quality assessment of urban green space under long-term reclaimed water irrigation. *Environ Sci Pollut Res* 23(5):4639–4649. <https://doi.org/10.1007/s11356-015-5693-y>
- Ministry of Environmental Protection of the People’s Republic of China (2002) Monitoring and analysis method of water and wastewater, 4th edn. China Environmental Science Press, Beijing, p 276 (in Chinese)
- Ministry of Land and Resources of the People’s Republic of China (2015) Standard for groundwater quality (DZ/T 0290–2015). Standards Press of China, Beijing (in Chinese)
- Mou S, Wang H, Sun Q (1993) Simultaneous determination of the three main inorganic forms of nitrogen by ion chromatography. *J Chromatogr A* 640(1–2):161–165. [https://doi.org/10.1016/0021-9673\(93\)80178-B](https://doi.org/10.1016/0021-9673(93)80178-B)
- Nash JE, Sutcliffe JV (1970) River flow forecasting through conceptual models part I—a discussion of principles. *J Hydrol* 10(3):282–290. [https://doi.org/10.1016/0022-1694\(70\)90255-6](https://doi.org/10.1016/0022-1694(70)90255-6)



- Pedrero F, Maestre-Valero JF, Mounzer O, Alarcón JJ, Nicolás E (2015) Physiological and agronomic mandarin trees performance under saline reclaimed water combined with regulated deficit irrigation. *AGR Water Manag* 146:228–237. <https://doi.org/10.1016/j.agwat.2014.08.013>
- Pereira BFF, He ZL, Stoffella PJ, Melfi AJ (2011) Reclaimed wastewater: effects on citrus nutrition. *AGR Water Manag* 98(12):1828–1833. <https://doi.org/10.1016/j.agwat.2011.06.009>
- Ramos TB, Simunek J, Gonçalves MC, Martins JC, Prazeres A, Castanheira NL, Pereira LS (2011) Field evaluation of a multi-component solute transport model in soils irrigated with saline waters. *J Hydrol* 407(1–4):129–144. <https://doi.org/10.1016/j.jhydrol.2011.07.016>
- Sanchez-Flores R, Conner A, Kaiser RA (2016) The regulatory framework of reclaimed wastewater for potable reuse in the United States. *Int J Water Resour D* 32(4):536–558
- Simunek J, Sejna M, Saito H, Sakai M, van Genuchten MTh (2008) The HYDRUS-1D software package for simulating the movement of water, heat, and multiple solutes in variably-saturated media. In: Version 4.0, HYDRUS software series 3. Department of Environmental Sciences, University of California Riverside, Riverside, p 315
- Simunek J, van Genuchten MT, Sejna M (2016) Recent developments and applications of the HYDRUS computer software packages. *Vadose Zone J* 15(7):1–25. <https://doi.org/10.2136/vzj2016.04.0033>
- Stolte J (1997) Determination of the saturated hydraulic conductivity using the constant head method. In: Stolte J (ed) Manual for soil physical measurements, technical document 37. DLO Winand Staring Centre, Wageningen
- Sun H, Mi F, Tian MH, Peng Q (2014) Risk assessment of water supply and demand for urban greening in Beijing. *Bull Soil Water Conserv* 34(5):1–6 (in Chinese)
- Tafteh A, Sepaskhah AR (2012) Application of HYDRUS-1D model for simulating water and nitrate leaching from continuous and alternate furrow irrigated rapeseed and maize fields. *AGR Water Manag* 113:19–29. <https://doi.org/10.1016/j.agwat.2012.06.011>
- Tran QK, Schwabe KA, Jassby D (2016) Wastewater reuse for agriculture: development of a regional water reuse decision-support model (RWRM) for cost-effective irrigation sources. *Environ Sci Technol* 50(17):9390–9399. <https://doi.org/10.1021/acs.est.6b02073>
- Twarakavi NKC, Simunek J, Seo S (2008) Evaluating interactions between groundwater and vadose zone using the HYDRUS-based flow package for MODFLOW. *Vadose Zone J* 7(2):757–768. <https://doi.org/10.2136/vzj2007.0082>
- United Nations Environment Programme (2015) Good practices for regulating wastewater treatment: legislation, policies and standards. <http://unep.org/gpa/documents/publications/GoodPracticesforRegulatingWastewater.pdf>. Accessed 17 Apr 2018
- United States Salinity Laboratory Staff (1954) Diagnosis and improvement of saline and alkali soils. In: Richards LA (ed) USDA handbook 60, Washington, DC
- van Genuchten MTh (1980) A closed form equation for predicting the hydraulic conductivity of unsaturated soils. *Soil Sci Soc Am J* 44:892–898
- van Genuchten MTh (1987) A numerical model for water and solute movement in and below the root zone, research report no. 121. US Salinity laboratory, USDA, ARS, Riverside
- van Genuchten MTh, Leij FJ, Yates SR (1991) The RETC code for quantifying the hydraulic functions of unsaturated soils, report no. EPA/600/2–91/065. R.S. Kerr Environmental Research Laboratory, US Environmental Protection Agency, Ada, p 85
- Wang YY (2011) Study on numerical simulation of groundwater recharge in plain area of Beijing. Master's thesis. Tsinghua University, Beijing (in Chinese)
- Wang XQ, Wang ZF, Qi YB, Guo H (2009) Effect of urbanization on the winter precipitation distribution in Beijing area. *Sci China Ser D* 52(2):250–256. <https://doi.org/10.1007/s11430-009-0019-x>
- Wang X, Daigger G, Lee DJ, Liu JX, Ren NQ, Qu JH, Liu G, Butler D (2018a) Evolving wastewater infrastructure paradigm to enhance harmony with nature. *Sci Adv*. <https://doi.org/10.1126/sciadv.aag0210>
- Wang Y, Song X, Li B, Ma Y, Zhang Y, Yang L, Bu H, Holm PE (2018b) Temporal variation in groundwater hydrochemistry driven by natural and anthropogenic processes at a reclaimed water irrigation region. *Hydrol Res* 49:1652–1668
- Waterloo Hydrogeologic Inc (2006) Visual MODFLOW professional user's manual. Waterloo Hydrogeologic Inc, Waterloo
- Xiao Y, Gu X, Yin S, Pan X, Shao J, Cui Y (2017) Investigation of geochemical characteristics and controlling processes of groundwater in a typical long-term reclaimed water use area. *Water* 9(10):800
- Xu ZF, Han GL (2009) Chemical and strontium isotope characterization of rainwater in Beijing, China. *Atmos Environ* 43(12):1954–1961. <https://doi.org/10.1016/j.atmosenv.2009.01.010>
- Xu P, Shao Y (2002) A salt-transport model within a land-surface scheme for studies of salinisation in irrigated areas. *Environ Model Softw* 17(1):39–49. [https://doi.org/10.1016/S1364-8152\(01\)00051-2](https://doi.org/10.1016/S1364-8152(01)00051-2)
- Xu X, Huang G, Zhan H, Qu Z, Huang Q (2012) Integration of SWAP and MODFLOW-2000 for modeling groundwater dynamics in shallow water table areas. *J Hydrol* 412–413:170–181. <https://doi.org/10.1016/j.jhydrol.2011.07.002>
- Yang ZQ (2007) Study of spatial-temporal variation characteristics of soil physicochemical properties affected by the irrigation with reclaimed water. *Prog Environ Sci Technol* 1:1420–1425
- Ye W, Wang H, Gao J, Liu H, Li Y (2014) Simulation of salt ion migration in soil under reclaimed water irrigation. *J Agro Environ Sci* 33(5):1007–1015 (in Chinese)
- Yuan XH, Teng WJ, Yang XJ, Wu JY (2009) Evapotranspiration and irrigation scheduling for three landscape ornamentals in Beijing, China. *N Z J Crop Hort* 37(3):289–294. <https://doi.org/10.1080/01140670909510275>
- Zhang ZY (2001) New green seedlings—Japan Euonymus. *For China* 8:25 (in Chinese)
- Zheng C, Wang P (1999) MT3DMS: a modular three-dimensional multispecies transport model for simulation of advection, dispersion, and chemical reactions of contaminants in groundwater systems. In: Documentation and user's guide, contract report SERDP-99-1. US Army Engineer Research and Development Center, Vicksburg
- Zhu Z, Dou J (2018) Current status of reclaimed water in China: an overview. *J Water Reuse Desalin*. <https://doi.org/10.2166/wrd.2018.070> (in press)
- Zhu Y, Shi LS, Lin L, Yang JZ, Ye M (2012) A fully coupled numerical modeling for regional unsaturated-saturated water flow. *J Hydrol* 475:188–203. <https://doi.org/10.1016/j.jhydrol.2012.09.048>